Optical resonances on sub-wavelength silver lamellar gratings

M. R. Gadsdon, I. R. Hooper and J. R. Sambles.

School of Physics, University of Exeter, Exeter, Devon, EX4 4QL, United Kingdom.

m.r.gadsdon@exeter.ac.uk

Abstract: The optical response of sub-wavelength silver lamellar gratings has been theoretically investigated. Two distinct types of resonance have been predicted for incident radiation with E-field perpendicular to the long axis of the wires. The first resonance has been identified as a cavity mode resonance that is associated with transmission enhancement. The second resonance has been identified as an entirely new horizontal plasmon resonance on the incident (and transmission) surfaces of the wires of the grating. Normal surface plasmon modes are investigated on discontinuous gratings, and their relation to those found on continuous gratings is highlighted by focusing on the perturbation effect of the discontinuities. It is shown that the new horizontal plasmon mode is in no way related to the well known diffractively coupled surface plasmon, and is shown to have a particle plasmon-like nature. It is therefore termed a *horizontal particle plasmon*, and may be either an *uncoupled horizontal particle plasmon* resonance (a 1-dimensional particle plasmon) or a *coupled horizontal particle plasmon* resonance (a 2-dimensional particle plasmon) depending on the height of the grating. It is shown that this resonance may result in a reflection efficiency that is very high, even when the grating would be optically thin if it were a homogeneous film, therefore, it behaves as an *inverse wire grid polariser* as it reflects more TM than TE incident radiation.

OCIS codes: (050.6624) Subwavelength Structures; (310.6628) Nanostructures; (240.6680) Surface Plasmons

References and links

1. R. W. Wood, "On the remarkable case of uneven distribution of light in a diffraction grating spectrum," Proc. R. Soc. London A **18**, 269–275 (1902).
2. U. Fano, "The Theory of Anomalous Diffraction Gratings and of Quasi-Stationary Waves on Metallic Surfaces (Sommerfelds Waves)," J. Opt. Soc. Am. **31**, 213–222 (1941).
3. H. Raether, *Surface Plasmons on smooth and rough surfaces and on gratings* (Springer-Verlag, Berlin, 1988).
4. Q. Cao and P. Lalanne, "Negative Role of Surface Plasmons in the Transmission of Metallic Gratings with Very Narrow Slits," Phys. Rev. Lett. **88**, 057403 (2002).
5. A. Barbara, E. Bustarret, T. López-Rios, P. Quémerais, and T. Fournier, "Electromagnetic resonances of sub-wavelength rectangular metallic gratings," Eur. Phys. J. D **23**, 143–154 (2003).
6. D. Crouse and P. Keshavareddy, "Role of optical and surface plasmon modes in enhanced transmission and applications," Opt. Express. **13**, 7760–7771 (2005).
7. J. A. Porto, F. J. Garcia-Vidal, and J. B. Pendry, "Transmission Resonances on Metallic Gratings with Very Narrow Slits," Phys. Rev. Lett. **83**, 2845–2848 (1999).
8. S. Collin, F. Pardo, R. Teissier, and J. Pelouard, "Horizontal and vertical surface resonances in transmission metallic gratings," J. Opt. A: Pure Appl. Opt. **13**, S154–S160 (2002).
9. H. Lochbihler, "Surface polaritons on metallic wire gratings studied via power losses," Phys. Rev. B **53**, 10289–10295 (1996).

#101954 - $15.00 USD Received 23 Sep 2008; revised 20 Nov 2008; accepted 23 Nov 2008; published 19 Dec 2008

10. A. P. Hibbins, J. R. Sambles, and C. R. Lawrence, "Gratingless enhanced microwave transmission through a subwavelength aperture in a thick metal plate," Appl. Phys. Lett. **81**, 4661–4663 (2002).
11. J. R. Suckling, A. P. Hibbins, M. J. Lockyear, T. W. Preist, J. R. Sambles, and C. R. Lawrence, "Finite Conductance Governs the Resonance Transmission of Thin Metal Slits at Microwave Frequencies," Phys. Rev. Lett. **92**, 147401 (2004).
12. I. R. Hooper and J. R. Sambles, "Dispersion of surface plasmon polaritons on short-pitch metal gratings," Phys. Rev. B **65**, 165432 (2002).
13. G. Schider, J. R. Krenn, W. Gotschy, B. Lamprecht, H. Ditlbacher, A. Leitner, and F. R. Aussenegg, "Optical properties of Ag and Au nanowire gratings," J. Appl. Phys. **90**, 3825–3830 (2001).
14. J. J. Burke, G. I. Stegeman, and T. Tamir, "Surface-polariton-like waves guided by thin, lossy metal films," Phys. Rev. B **33**, 5186–5201 (1986).
15. E. N. Economou, "Surface Plasmons in Thin Films," Phys. Rev. **182**, 539–554 (1969).
16. J. P. Kottmann and O. J. F. Martin, "Plasmon resonant coupling in metallic nanowires," Opt. Express. **8**, 655–663 (2001).
17. J. P. Kottmann, O. J. F. Martin, D. R. Smith, and S. Schultz, "Plasmon resonances of silver nanowires with a nonregular cross section," Phys. Rev. B **64**, 235402 (2001).
18. J. P. Kottmann and O. J. F. Martin, "Influence of the cross section and the permittivity on the plasmon-resonance spectrum of silver nanowires," Appl. Phys. B **73**, 299–304 (2001).
19. M. Moskovits, "Surface-enhanced spectroscopy," Rev. Mod. Phys. **57**, 783–826 (1985).
20. C. Y. Chen and E. Burstein, "Giant Raman Scattering by Molecules at Metal-Island Films," Phys. Rev. Lett. **45**, 1287–1291 (1980).
21. M. G. Moharam and T. K. Gaylord, "Rigorous coupled-wave analysis of metallic surface-relief gratings," J. Opt. Soc. Am. A **3**, 1780–1787 (1986).
22. L. Li, "Formulation and comparison of two recursive matrix algorithms for modeling layered diffraction gratings," J. Opt. Soc. Am. A **13**, 1024–1035 (1996).
23. D. Nash and J. R. Sambles, "Surface plasmon - polariton study of the optical dielectric function of silver," J. Mod. Opt. **43**, 81–91 (1996).
24. M. Honkanen, V. Kettunen, M. Kuittinen, J. Lautanen, J. Turunen, B. Schnabel, and F. Wyrowski, "Inverse metal-stripe polarizers," Appl. Phys. B **68**, 81–85 (1999).
25. J. A. Stratton *Electromagnetic Theory*, (John Wiley and Sons Inc, New Jersey, 2007).
26. R. F. Harrington and D. T. Auckland, "Electromagnetic Transmission Through Narrow Slots in Thick Conducting Screens," IEEE Trans. Antennas Propag. **AP-28**, 616–622 (1980).
27. Y. Takakura, "Optical Resonance in a Narrow Slit in a Thick Metallic Screen," Phys. Rev. Lett. **86**, 5601–5603 (2001).

1. Introduction

Thick metal films, which have small periodic perturbations, do not have the same optical response as that associated with a planar mirror made of the same material. This has long been understood as a result of the emergence of diffracted orders and the excitation of surface plasmon polaritons [1–3].

Metallic lamellar gratings, gratings consisting of a periodic array of metallic wires whose periodicity is the same or greater than the wavelength of the incident radiation, have been an area of considerable interest in recent years. These have been investigated, both experimentally and theoretically, for a range of different metals and for a section of the electromagnetic spectrum ranging from the infrared [4–9] through to the microwave regime [10, 11]. These well known surface plasmons have been termed *horizontal surface plasmons* [8]. It had been thought that surface plasmons could not be excited in the sub-wavelength regime, where the periodicity is significantly less than the wavelength of the incident radiation. However it has been shown that surface plasmons may be excited on sub-wavelength gratings if they form cavity modes in the slits of the structure.

Such cavity modes have been investigated in closed bottom structures (surface relief gratings) with a gaussian groove cross section [12], where they have been shown to arise from the evolution of the surface plasmon standing waves that occur on shallow gratings where, as the grating is made deeper, the surface plasmons on the groove walls may couple together across the slit. These have been termed *vertical surface plasmons* [8]. They have also been observed

#101954 - $15.00 USD Received 23 Sep 2008; revised 20 Nov 2008; accepted 23 Nov 2008; published 19 Dec 2008

in the microwave regime for a single slit [10] and for an array of slits [11], and in the infra-red regime for lamellar gratings with narrow slits [4–8].

This report presents an investigation of two resonant features of sub-wavelength metallic lamellar gratings, mainly focusing on the visible regime. The first feature is associated with enhanced transmission and is of the same nature as that observed in the lower energy part of the electromagnetic spectrum - simple cavity modes. The second feature is an entirely new horizontal particle plasmon resonance and is associated with a significant increase in the *reflection* response of such gratings.

With a small numbers of exceptions [4, 6], previous studies have associated horizontal surface plasmon resonances on diffractive gratings with an increase in transmission. However, because a new horizontal plasmon resonance is presented, which is associated only with an increase in reflection, there is a chance that readers may assume that the present work is joining one of the previous pieces of work commenting for or against enhanced transmission by normal diffractively coupled horizontal surface plasmons. It is emphasised that the horizontal resonance discussed is an entirely new horizontal resonance, that is in no way related to the normal diffactively excited horizontal surface plasmon, and hence the present work does not make any comment on the nature of enhanced transmission by such surface plasmons. Furthermore, as the new horizontal resonance presented may occur in the non-diffactive regime, while the well known diffractively excited horizontal surface plasmon resonance cannot, the work largely discusses non-diffractive structures in order to avoid any confusion between the two.

For very thin gratings, it is possible for this resonance to cause strong reflection of radiation polarised perpendicular to the wires, where it would normally be expected that the film would be optically thin. This leads to the structures reflecting more TM radiation than they transmit, and vice versa for TE, such that the structrues behave as *inverse* wire grid polarisers. We believe this new resonance has been observed experimentally to date [13] but not fully explained.

When the thickness of a semi-infinite metallic film is of the order of or smaller than the decay length of the evanescent field of the surface plasmon polariton in the metal, then surface plasmon polaritons on the top and bottom surfaces of the film may become coupled. This coupling may be either antisymmetric or symmetric, that is the tangential magnetic field (the magnetic field in the plane of the surface and perpendicular to the propagation direction of the surface plasmon polariton) may show a zero inside the metal film or it may not, respectively [14]. These two modes split into a higher frequency (antisymmetric) and a lower frequency (symmetric) resonance [15]. It should be noted that, when the dielectric media on either side of the film are not the same, the coupling is no longer exactly symmetric/antisymmetric. As the thickness of the film decreases, the higher frequency resonance increases in frequency away from the uncoupled surface plasmon resonance while the low frequency resonance decreases. For the symmetric mode, as the thickness of the metal film decreases, the amount of field that penetrates into the metal also decreases. Therefore, the absorption loss associated with this field penetration decreases and the coupled mode may propagate further - a long range surface plasmon polariton. Conversely, for the asymmetric case, as the metal thickness decreases, more of the field penetrates into the metal and its propagation length decreases - a short range surface plasmon polariton.

There has also been an examination of the optical response of individual, and coupled, wires with a variety of shapes, from simple circular cross-sections [16] to more complex irregular cross-sections [17, 18]. Under TM illumination in the classical mount, these wires exhibit an optical response that is analogous with the optical responses of particle plasmons [19, 20]. Therefore, these resonances typically behave as optical dipoles, where the re-radiation of light is not necessarily in the same direction as the specularly reflected light. As such, their response is typically characterised by the scattering cross-section and transmission extinction.

#101954 - $15.00 USD Received 23 Sep 2008; revised 20 Nov 2008; accepted 23 Nov 2008; published 19 Dec 2008

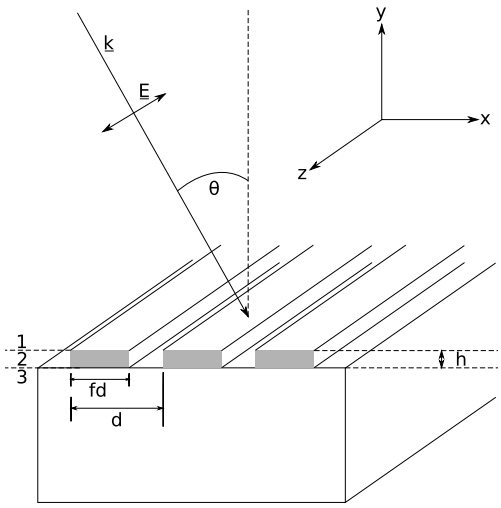

Fig. 1. Schematic representation of the theoretical model.

2. Theoretical model

All of the modelling in the present work utilises the rigorous coupled-wave analysis technique, also called the Fourier modal method [21]. In this technique the system is split into three regions as in Fig. 1. The permittivity profile in the *x*-direction is approximated as a Floquet series expansion. In each region the electromagnetic wave is described as the superposition of "*upward*" and "*downward*" waves in the *y*-direction. Each of these waves is then described as a Rayleigh expansion of eigenmodes, each of which is also expanded according to the Floquet series expansion associated with the approximation of the permittivity profile. Maxwell's equations are explicity solved in each region according to the description above of the electromagnetic fields. The resultant solutions are then used to match the electromagnetic boundary conditions, at the interface between each region, using the numerically stable scattering matrix [22]. The convergence of the calculations, as a function of the number of Fourier components used in the decomposition of the fields and grating profile, was verified for each calculation and was always in excess of $N = \pm 100$.

Figure 1 gives a schematic representation of the model used in this work. Region 2 is a lamellar grating consisting of silver and air with grating height, *h*, period, *d*, and mark-to-space ratio, *f*. Region 1, the incidence medium, is air and region 3, the transmission medium, is glass with refractive index $n_{glass} = 1.52$ unless otherwise stated. The incident radiation is at an angle θ to the interface normal with the incident plane containing the grating vector. It is linearly polarised with the E-field perpendicular to the long axis of the grating wires, TM (in the plane of incidence), unless otherwise stated. All calculations are made at normal incidence except for Figs. 13 and 9 where θ is allowed to vary.

The permittivity of silver is specified by the Drude model, using the parameters $\omega_p = 1.32 \times 10^{16}\ s^{-1}$ and $\tau_D = 1.45 \times 10^{-14}\ s$, taken from Nash and Sambles [23]. One needs to be aware that the permittivities in the case of a thin 2-dimensional wire may be different from those of an infinite film. It has been discussed elsewhere that the classical macroscopic approach of electrical permittivity is adequate for particle dimensions as small as 2 *nm* [17]. As a bulk metal is reduced in thickness towards this value, the mean free path of the electrons decreases as the electron surface scattering becomes more important. However, it has been shown that, for such silver wires as studied here, only the imaginary part of the permittivity increases slightly [18].

#101954 - $15.00 USD Received 23 Sep 2008; revised 20 Nov 2008; accepted 23 Nov 2008; published 19 Dec 2008

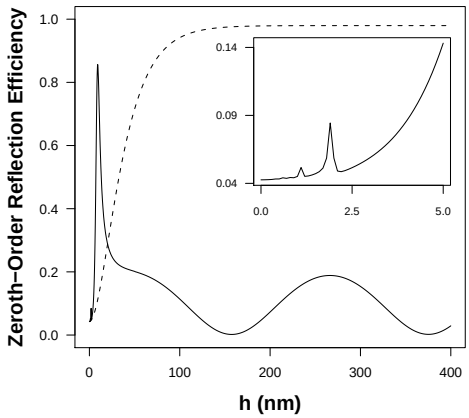

Fig. 2. Reflection efficiency as a function of grating height, h, for the parameters $d = 144\ nm$, $f = 0.45$, $\lambda = 550\ nm$. The inset gives an enlarged view of the region $0\ nm \leq h \leq 5\ nm$. The solid line gives the response to radiation with E-field parallel to the grating vector, while the dashed line gives the response to radiation with E-field perpendicular to the grating vector.

Thus, it is the present authors' belief that the underlying physics presented here is sound and that the changes in permittivity will only result in a slight broadening and reduction in magnitude of the resonances.

3. Initial results

Figure 2 gives the predictions of the specularly reflected efficiency as a function of grating height of an incident (in air) plane wave, of wavelength, $\lambda = 550\ nm$, upon a grating of period $d = 144\ nm$, with $f = 0.45$ and $\theta = 0^0$. There are clearly two types of resonances. One type of broad resonance is associated with zeros in reflection and appears to be periodic with grating height. The other, sharper type of resonance, gives reflection enhancement and only appears at very small values of the grating height. There is a weaker higher order mode at $h = 2\ nm$ (see inset of Fig. 2). Also presented is the reflection efficiency of radiation with its E-field parallel to the long axis of the wires (TE). At small grating thicknesses the grating reflects more radiation with E-field perpendicular to the wires than that with E-field parallel, and hence is acting in the opposite sense to that which is expected.

4. Resonance dependence

4.1. Dependence of modes with grating height

Figure 3 is a plot illustrating how the resonances depend spectrally on the height of the grating h. Figure 2 equates to the horizontal section of Fig. 3 at a frequency of $\omega = 2\pi c/\lambda = 3.42 \times 10^{15}\ rad.s^{-1}$. It should be noted that in all subsequent plots, showing the dependence of the resonances of the structure on different parameters, it is assumed that the max/minima of the reflection curves are very close to the resonant frequency, which is given by the poles of the scattering matrix, S.

In Fig. 3 it can be seen that the two resonances behave very differently with increasing h. Although they cross, there does not appear to be any interaction between the two, as they do

#101954 - $15.00 USD Received 23 Sep 2008; revised 20 Nov 2008; accepted 23 Nov 2008; published 19 Dec 2008

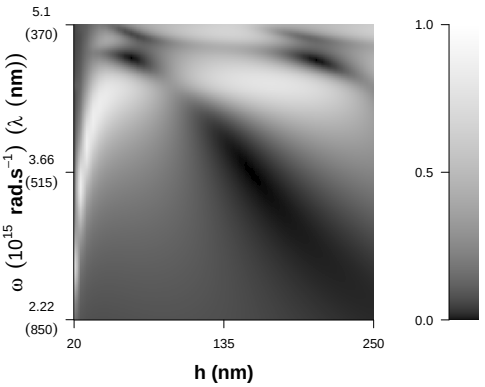

Fig. 3. Reflection efficiency response of the grating as a function of both the incident frequency and grating height. The fixed grating parameters are $d = 144$ *nm*, $f = 0.45$. The wavelength range is $370\ nm \leq \lambda \leq 850\ nm$, which equates to a frequency range of $2.22 \times 10^{15}\ rad.s^{-1} \leq \omega \leq 5.10 \times 10^{15}\ rad.s^{-1}$. The grating height is in the range $20\ nm \leq h \leq 240\ nm$.

not show anti-crossing behaviour, and the resulting reflection efficiency is an average of the two responses.

We first examine the behaviour of the sharp resonance associated with reflection enhancement, as a function of grating height. Figure 4 gives an enlarged view of the response in the region $5\ nm \leq h \leq 40\ nm$. This resonance blueshifts as the grating height is increased from approximately $h = 5$ *nm* to $h = 40$ *nm*, at which point the resonance then becomes independent of further increases of h. We note that the decay length of an SPP at 420 *nm* in silver is approximately 25 *nm*, and yet the reflection efficiency associated with this resonance may be in excess of 0.8 when the grating height is below this value; where one would expect a continuous film to start becoming transparent. This leads to the interesting effect that the grating acts as an *inverse polariser* [24] because the grating is becoming optically thin with regards to TE polarisation, but highly reflective for TM polarisation. Also note than alternative device with an interesting response is possible for wires that are not optically thin, at this point the structure behaves as a standard polariser, except at certain frequencies, where it reflects all polarisations and behaves as a simple mirror.

The magnitude of the $|H_z|$-field, for one unit cell, is plotted for the reflection peak ($h = 9.5$ *nm*) in Fig. 5(a). The black line outlines the location of one of the silver grating wires. It can be seen that the grating is sufficiently thin to allow the evanescent fields of horizontal plasmons that are excited on the upper face of the array to excite and couple to a secondary horizontal plasmon on the lower surface, *through the metal*. The different field strengths of the upper and lower horizontal plasmons are due to the fact that this is an asymmetric structure because the refractive indices of the incident and transmission media are not the same. Also note that the fields are well localised to each wire in the x-direction, with little field strength penetrating beyond approximately 15 *nm* into the dielectric in the slit. Figure 5(b) shows the equivalent field plot for the higher order resonance at $h = 2$ *nm*, note the different scales such that the field enhancement is much less than for the fundamental mode.

The field plots for the reflection enhancing mode indicate that the very thin wire is acting like a particle plasmon [19, 20], except that it is a *2-dimensional* particle plasmon. In this interpretation, the fundamental resonance is equivalent to a dipolar resonance, while the higher

#101954 - $15.00 USD Received 23 Sep 2008; revised 20 Nov 2008; accepted 23 Nov 2008; published 19 Dec 2008

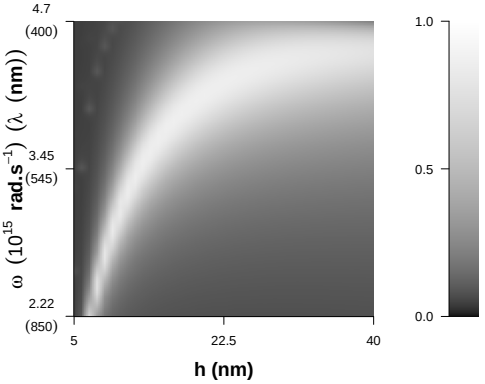

Fig. 4. Reflection efficiency response of the grating as a function of both the incident frequency and grating height. The fixed grating parameters are $d = 144$ *nm*, $f = 0.45$. The frequency range is $2.22 \times 10^{15}\ rad.s^{-1} \leq \omega \leq 4.7 \times 10^{15}\ rad.s^{-1}$, which equates to a wavelength range of $400\ nm \leq \lambda \leq 850\ nm$. The grating height is in the range $5\ nm \leq h \leq 40\ nm$.

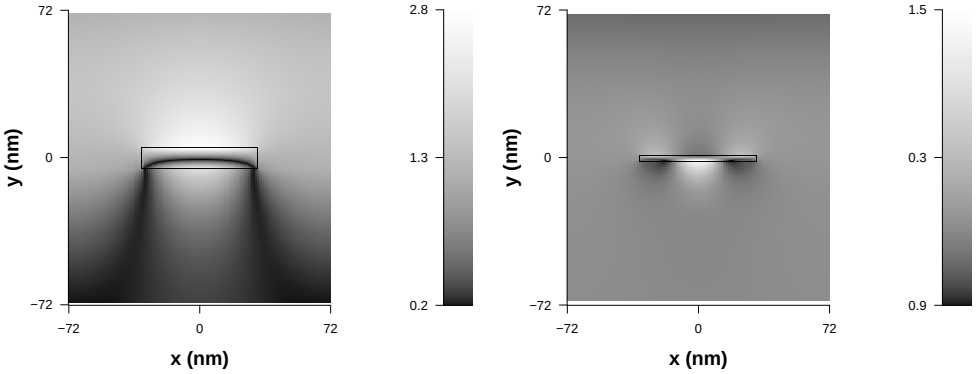

(a) $h = 9.5\ nm$ (b) $h = 2\ nm$

Fig. 5. $|H_z|$ for the two reflection peaks at low grating thickness in Fig. 2, with $d = 144$ *nm*, $f = 0.45$, $\lambda = 550$ *nm*.

#101954 - $15.00 USD Received 23 Sep 2008; revised 20 Nov 2008; accepted 23 Nov 2008; published 19 Dec 2008

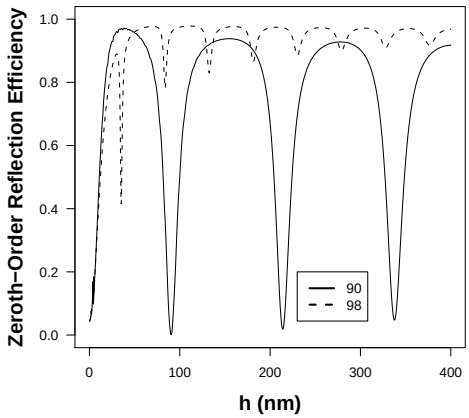

Fig. 6. Reflection efficiency as a function of grating height for two high f values. The grating parameters are $d = 144$ *nm*, $f = 0.9$ and $f = 0.98$, $\lambda = 550$ *nm*.

order mode is a multi-polar resonance [13]. Therefore, the suggestion is that this resonance is essentially the same as the resonance found previously on individual wires with different cross-sections [16–18]. However, what makes this resonance subtly distinct, from the particle plasmon resonances described in previous work (where light is re-radiated in a variety of directions), is that the planar structure and periodicity of the wires causes the re-radiated light to propagate in the same direction, and with the same phase, as the specularly reflected radiation. Therefore, a reflection enhancement occurs and the response can be fully described by the transmission, reflection, and absorption, rather than by the scattering cross-section. It is this effect that allows the grating to behave as an inverse wire grid polariser, which may be useful for optical devices.

Field plots of the horizontal plasmon resonance in the flat banded region are almost identical to those in Fig. 5(a), except that the field enhancement is slightly weaker. Therefore, the coupling that occurs for low grating heights causes an enhancement in the field strengths of the resonance as well as a redshift. We call the low grating thickness resonance, a *coupled horizontal particle plasmon* and the resonance at large grating thickness an *uncoupled horizontal particle plasmon*. Thus, the coupled resonance may be thought of as a 2-dimensional particle plasmon, while the uncoupled resonance is effectively a 1-dimensional particle plasmon.

We now consider the two reflection minima in Fig. 2 at $h \approx 160$ *nm* and $h \approx 375$ *nm*, which are associated with cavity mode resonances in the slits between the wires [10]. By increasing the mark-to-space ratio f (the fraction of a period that is metal, and hence narrow the slits) it is possible to sharpen these resonances, as shown in Fig. 6:

In fact, Fig. 6 illustrates that, as the slits of the grating are narrowed, the resonance not only sharpens, but it redshifts considerably. As the slits becomes very thin ($f = 0.9 \rightarrow slit\ width = 14.4\ nm$), it is possible to fit a 550 *nm* incident wavelength into a 91 *nm* wide slit and still achieve ≈ 0 reflection efficiency. Decreasing the slit beyond this causes the modes to redshift to a greater extent, however, there is significant increase in reflection (and hence loss of transmission).

Figure 7(a) gives the magnitude of the $|H_z|$-field, for one unit cell, for the case of very narrow slits where $d = 144$ *nm*, $f = 0.9$, $\lambda = 550$ *nm*, note the increase in the maximum field enhancement from ~ 3 in Fig. 5 to ~ 7 in Fig. 7. The fundamental resonance at $h = 91$ *nm* is shown in Fig. 7(a), as is the first harmonic resonance at $h = 215$ *nm* in Fig. 7(b). From these

#101954 - $15.00 USD Received 23 Sep 2008; revised 20 Nov 2008; accepted 23 Nov 2008; published 19 Dec 2008

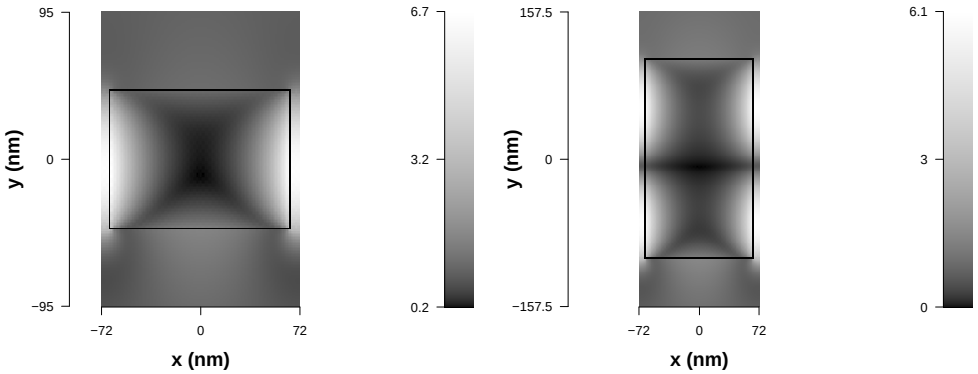

(a) $h = 91\ nm$ (b) $h = 215\ nm$

Fig. 7. $|H_z|$ for the two reflection minima of Fig. 6, with $d = 144\ nm$, $f = 0.9$, $\lambda = 550\ nm$.

field plots it is clear that the periodic reflection extinctions, observed in Figs. 3 and 6, are due to the excitation of cavity modes in the slits of the grating, analogous to those discussed in Hooper and Sambles [12], except with the different boundary conditions of a slit compared to a deep groove.

Figure 3 illustrates that the frequency dependence of the cavity modes is highly asymmetric with grating height. It can be observed in Fig. 3 that, for longer wavelengths, the cavity modes are free to decrease in frequency approximately as $1/h$ as one would expect. However, Fig. 3 also demonstrates that the high frequency cavity modes are not able to increase in frequency linearly with decreasing grating height. Each mode may not increase in frequency beyond its associated light line and we observe an anti-crossing between a low-order high energy branch and a high-order low energy branch [7, 12] at approximately $\lambda = 400\ nm,\ \omega = 4.7 \times 10^{15}\ rad.s^{-1}$. It is this behaviour that shows that these cavity modes are actually subtly distinct from the familiar TEM cavity mode in a single slit, which would increase in frequency with decreasing grating height for all heights/frequencies (this is only strictly true for a perfect conductor [11]). This is because, as discussed in the Introduction, on a grating the cavity modes evolve directly from diffractively coupled surface plasmon modes, which become vertical surface plasmons that self couple across the walls of the slits. This is possible even for non-diffractive structures due to the significant perturbation to the dispersion of the normal surface plasmons on shallow gratings, which the large amplitude grating introduces [8, 12].

In order to confirm the nature of these two resonances, the horizontal particle plasmon resonances and cavity modes, which may also be thought of as vertical surface plasmon resonances coupled across the slit, it is instructive to also observe how they depend on wire and slit width and on the in-plane momentum of the incident radiation.

4.2. Dispersion of cavity resonance with slit width and in-plane momentum

We briefly confirm that the reflection minima are associated with cavity modes by observing that they behave with varying slit width and in-plane momentum as expected. In Fig. 8 we give the dependence of the cavity mode ($h = 91\ nm$) on the slit spacing from 10 *nm* to 100 *nm* with a constant wire width of *129.6 nm*. As the slit width is increased from very thin values the resonance blueshifts. This thin slit width behaviour has been observed previously for a single slit in the microwave regime and has been attributed to the finite penetration depth of

#101954 - $15.00 USD Received 23 Sep 2008; revised 20 Nov 2008; accepted 23 Nov 2008; published 19 Dec 2008

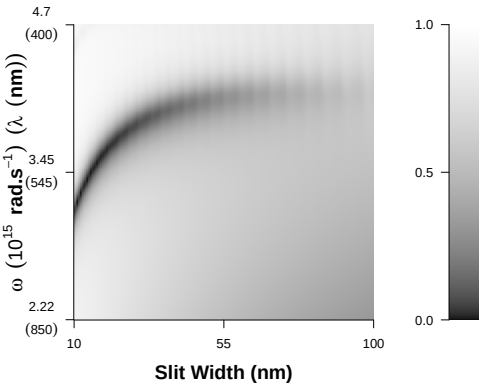

Fig. 8. Reflection efficiency response of the cavity mode resonance as a function of both the incident frequency and slit width, for a constant wire width of 64.8 *nm*. The grating height is $h = 91$ *nm*. The frequency is in the same range as in Fig. 4 and the slit width is in the range $10\ nm \leq slit\ width \leq 100\ nm$.

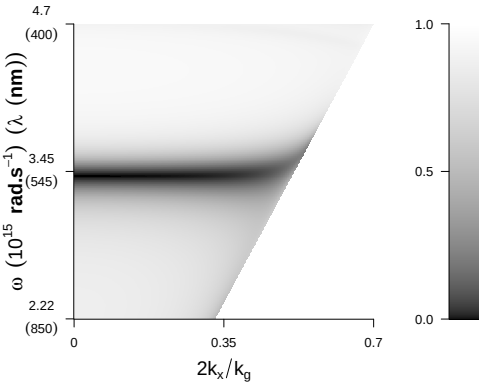

Fig. 9. Reflection efficiency response of the cavity mode resonance as a function of both the incident frequency and in-plane momentum. The grating parameters are $h = 91$ *nm*, $d = 144$ *nm* and $f = 0.9$. The frequency is in the same range as in Fig. 4 and the in-plane momentum is in the range $0 \leq 2k_x/k_g \leq 1$.

the evanescent fields in the metal. At large slit widths the standing wave may be considered as approximately a plane wave-front, whereas, when the slit width is reduced, the finite penetration depth in the metal induces an increase in the imaginary k_x, which in turn increases the curvature of the wave-front [11]. For increases in slit width one would expect a down turn in the resonant frequency as this effect decreases and changes in the boundary conditions due to end effects start to dominate [26,27]. However, beyond a slit width of approximately 50 *nm* the cavity mode is very weak and diminishes quickly with increasing slit width, therefore, it is not possible to observe this effect at large slit width in the optical regime.

The dependence of the cavity mode on the in-plane momentum, shown in Fig. 9, behaves similarly to those previously observed, both in continuous surface relief gratings [12] and lamellar gratings [4–8]. In narrow slits the strong coupling of the vertical SPPs across the slits induces

#101954 - $15.00 USD Received 23 Sep 2008; revised 20 Nov 2008; accepted 23 Nov 2008; published 19 Dec 2008

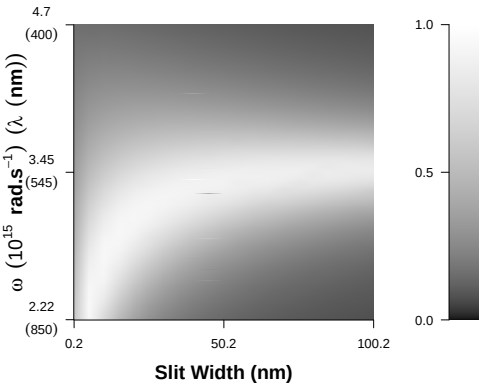

Fig. 10. Reflection efficiency response of coupled horizontal particle plasmon resonance as a function of both the incident frequency and slit width, for a constant wire width of 64.8 *nm*. The grating height is $h = 9.5$ *nm*. The frequency is in the same range as in Fig. 4. The slit width is in the range $0.2\ nm \leq (1-f)d \leq 100.2\ nm$.

the opening of very large bands gaps, which results in a flat banded dispersion curve. These flat bands interact with the free radiation, whose density of states becomes divergent at grazing incidence [12], and the flat bands strongly anti-cross with the light line at large angles of incidence. The interaction of the flat SPP bands with the light line highlights another subtle difference between a TEM cavity mode and a periodic array of slits.

There is a slight decrease in the magnitude of the reflection extinction at the higher angles of incidence. The total reflection efficiency is a superposition of the directly reflected radiation and that which is reradiated by the surface plasmon/cavity modes. In an analogy with the Brewster Angle at a dielectric interface, at grazing angles on a dielectric metal interface, the directly reflected radiation is of a different phase to that reflected near normal incidence [25]. Therefore the slight reduction in reflection extinction at large k_x is due to the reradiated radiation from the cavity mode not having the same phase difference to the directly reflected radiation at grazing angles as it does near normal incidence.

4.3. Dependence of horizontal plasmon resonance with wire width, slit width and in-plane momentum

In order to show that the horizontal particle plasmon resonances are new resonances, and not, for example, a combination of normal diffractively excited surface plasmons and the observed cavity modes, we continue to use sub-wavelength structures, so that normal surface plasmons are not diffractively excited. In addition we focus on the coupled horizontal particle plasmon mode because it only occurs on very thin structures, where cavity modes cannot exist.

Figure 10 is a plot demonstrating the spectral dependence of the coupled horizontal particle plasmon resonance ($d = 144$ *nm*, $h = 9.5$ *nm*) for a constant wire width of 64.8 *nm* and varying slit width from 0.2 *nm* to 100.2 *nm*. The resonance is independent of the slit width above 30 *nm*, whereas below this slit width, the resonance rapidly decreases in frequency and broadens. This is interpreted as the *localised* horizontal particle plasmons being able to interact across the narrow slits, in a manner similar to how the resonances of particle plasmons shift when individual particles become close enough to interact. Further support of this effect is evident when one considers the fact that, in the *x*-direction, Fig. 5(a) shows that the fields penetrate into the dielectric for approximately 15 *nm*. The large grating height (uncoupled) horizontal particle

#101954 - $15.00 USD Received 23 Sep 2008; revised 20 Nov 2008; accepted 23 Nov 2008; published 19 Dec 2008

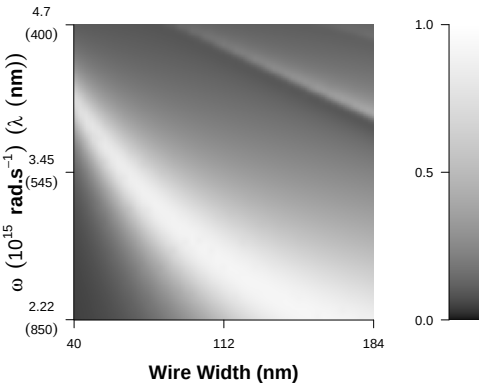

Fig. 11. Reflection efficiency response of the coupled horizontal particle plasmon resonance as a function of both the incident frequency and wire width, for a constant slit width of 79.2 *nm*. The grating height is $h = 9.5$ *nm*. The frequency is in the same range as in Fig. 4. The wire width is in the range 40 $nm \leq fd \leq 184$ *nm*.

plasmon resonance depends similarly on wire width.

Figure 11 gives the spectral dependence of the same resonance, this time for a fixed slit width of 79.2 *nm* while varying the wire width from 40 *nm* to 184 *nm*. The resonance frequency behaves as $1/fd$ as the width of the wires (fd) is increased. The secondary, weaker, resonance toward the upper right corner is of the same nature as shown in Fig. 5(b), illustrating that it is possible to obtain the higher order mode at a more practicable thickness. This linear redshift with varying wire width accords with the suggestion that the mode is localised to the wires of the structure.

Figure 12 gives a slight variation on these two investigations, here the period of the grating is held at a constant 144 *nm* while the mark-to-space ratio is varied from 0.2 to 0.8. This results in both the wire width and slit width changing concurrently, however, the slit width is always kept above 30 *nm* and so, from Fig. 10, we expect this to have no effect on the response. Again, we see a $1/fd$ dependence of the resonance with wire width. In this case the period is held constant, yet the resonance depends on wire width, whereas, in Fig. 10 the resonance is independent of slit width (for constant wire width) and hence changing period. Therefore we conclude that the coupled horizontal particle plasmon resonance on lamellar gratings is *not* the same as the well known diffractively excited surface plasmon resonance that arises on continuous surface relief gratings, which obeys Equation 1, and is dependent on the period of the grating.

$$k_{sp} = k_0 sin(\theta) \pm qk_g \tag{1}$$

where k_{sp} is the surface plasmon momentum, k_0 is the incident radiation momentum, k_g is the grating vector, and q is any integer.

Figure 13 is a plot showing how the fundamental coupled horizontal particle plasmon resonance ($d = 144$ *nm*, $f = 0.45$, $h = 9.5$ *nm*) depends spectrally on the in-plane momentum k_x. This result is another example of how the localised horizontal particle plasmons presented here behave differently to the well known normal surface plasmon polaritons that are excited by diffractive continuous surface relief gratings (which are not confined to each of the grating wires by the slits and may propagate between surface perturbations). In the latter case it is well known that the dispersion of the mode with k_x follows the dispersion of a surface plasmon

#101954 - $15.00 USD Received 23 Sep 2008; revised 20 Nov 2008; accepted 23 Nov 2008; published 19 Dec 2008

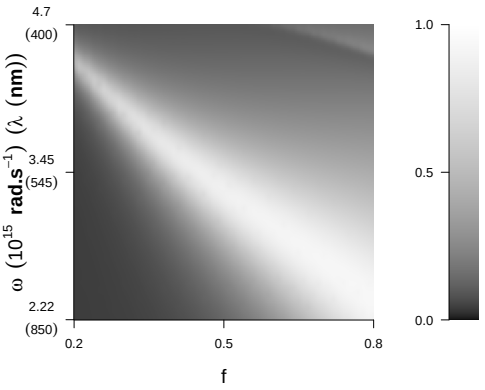

Fig. 12. Reflection efficiency response of the coupled horizontal particle plasmon resonance as a function of both the incident frequency and mark-to-space ratio, for a constant grating period of 144*nm*. The grating height is $h = 9.5$ *nm*. The frequency is in the same range as in Fig. 4. The mark-to-space ratio is in the range $0.2 \leq f \leq 0.8$, giving a slit width that is always ≥ 28.8 *nm*.

polariton on a flat surface that has been band folded by the periodic translational variance of the grating. Here we show that, in the case of the localised horizontal particle plasmons that may be formed on a discontinuous grating, there is no dependence of the spectral position of the resonance on the angle of incidence. This independence of the resonance with k_x has been observed previously for particle plasmons as well as other localised modes. Field plots show that the nature of the resonance does not significantly alter with the angle of incidence. As with the results of the dependency on wire and slit width, this result confirms the localisation of the resonance to the surface of the wires, rather than being able to propagated freely between perturbations, as is the case on a continuous grating, and hence its distinctness from the latter. This localisation also demonstrates that these modes may also be excited on individual wires as well as arrays.

As for the dependence of the cavity modes, the reduction of the reflection efficiency, to the point where the grating becomes almost transmissive at grazing angles is attributed to a pseudo-Brewster angle.

Similar investigations into the uncoupled horizontal particle plasmon resonance (the large h high reflection resonance) illustrate that this resonance depends on wire width, slit width, period, and in-plane momentum in the same way as the small h coupled resonance.

5. Surface plasmon modes on discontinuous gratings and the origin of the particle plasmon mode

For surface plasmons on continuous gratings it has been shown that, as the grating amplitude is increased, the unperturbed resonances may be scattered such that they self-interact to form localised modes within the deep grooves of the structure which behave as cavity modes [12]. Therefore, it is possible that the localised horizontal particle plasmon modes formed on discontinuous gratings may also be the result of an evolution of normal surface plasmons as the confinement of a discontinuous grating is introduced. In order to interpret the following results correctly, it is important to first highlight the perturbation effects that the discontinuities of a lamellar grating can have on the dispersion of the normal surface plasmon polariton resonance; which is also an interesting investigation in its own right, and to the Authors' knowledge, has

#101954 - $15.00 USD Received 23 Sep 2008; revised 20 Nov 2008; accepted 23 Nov 2008; published 19 Dec 2008

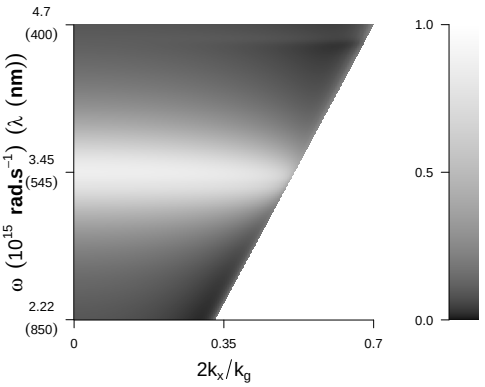

Fig. 13. Reflection efficiency response of the coupled horizontal particle plasmon resonance as a function of both the incident frequency and in-plane momentum. The grating parameters are $d = 144\ nm$, $f = 0.45$ and $h = 9.5\ nm$. The frequency is in the same range as in Fig. 4 and the in-plane momentum is in the range $0 \leq 2k_x/k_g \leq 1$.

not been examined in detail on lamellar gratings in the optical regime. This briefly requires a shift to diffractive structures.

In order to investigate in more detail the evolution of the particle plasmon resonance a more complex system is modelled. The system is identical to the schematic shown in Fig. 1, except that a new layer is introduced between the grating and the transmission (substrate) layers. This is a homogeneous silver layer of thickness *t*, such that when this layer is optically thick, the structure resembles a continuous surface relief grating, and when this layer has zero thickness, the structure is identical to a discontinuous structure. Therefore, the variation of the thickness of this layer allows the examination of the evolution of the resonances as the structure tends from a continuous to a discontinuous one.

It is clear that a surface plasmon on a continuous grating with a rectangular profile of small amplitude will occur at the same frequency as that expected from any continuous diffraction grating with a small perturbation e.g. a sinusoidal grating. If the grating amplitude is not small then it will perturb the surface plasmon propagation significantly, resulting in the frequency and dispersion of the mode being modified. It has been shown that increasing the grating height, increasing the perturbation to the surface plasmon mode, results in a flattening of the dispersion diagram along with a redshift in frequency [12]. However, unlike a sinusoidal grating, a rectangular grating with a large amplitude, but also very narrow grooves, will also allow unperturbed surface plasmons to exist on its upper surface. This is because it approximates a homogeneous interface, and so does not significantly disturb the surface plasmon propagation, while the periodicity still allows diffractive coupling. Likewise, an optically thick, discontinuous rectangular grating with very narrow slits will also allow unperturbed surface plasmons to exist on its upper surface. Thus large amplitude rectangular gratings, either continuous or discontinuous, with very narrow grooves/slits will support very similar optical resonances, they will both allow normal surface plasmon modes and cavity modes to exist on them, although the cavity modes on the continuous grating will occur at approximately twice the wavelength of the discontinuous grating due to the different boundary conditions of the ground plane. However, this is not the case for lamellar gratings with a small height.

As described in the Introduction, for homogeneous films, if the height of the film is reduced below the decay length of the evanescent fields of the surface plasmons in the metal, then

#101954 - $15.00 USD Received 23 Sep 2008; revised 20 Nov 2008; accepted 23 Nov 2008; published 19 Dec 2008

the evanescent fields associated with the surface plasmon on the upper surface will be able to excite surface plasmons on the bottom surface. The upper and lower surface plasmons then become coupled, resulting in a splitting of the normal surface plasmon mode into the long range and short range coupled surface plasmon resonance, which disperse in frequency in opposite directions with further decreases in grating height. This will also be true for thin discontinuous gratings with very narrow slits. Figure 14 demonstrates the evolution of normal surface plasmon modes to coupled normal surface plasmon modes, on a grating with narrow slits, as the grating tends from a continuous one to a discontinuous one by starting with a large t and reducing it to zero. They are plots of the poles of the scattering matrix, which are determined by summing over all of the global scattering matrix, S. This technique leads to very sharp and large peaks, thus for ease of visualisation, in each plot the poles are normalised to the maximum value obtained in the given plot, $(\sum|S|)_{max}$, giving a range $0 \leq \sum|S| / (\sum|S|)_{max} \leq 1$, and the grey-scale set between 0 and 0.5. The pole plots show the dispersion of the modes as the height of the metal substrate layer is reduced from $t = 64$ *nm* (almost optically thick so that the grating is almost continuous) to $t = 0$ *nm*, where the grating is fully discontinuous. The grating parameters are: $h = 10$ *nm*, $d = 500$ *nm*, $fd = 480$ *nm*, and the substrate is vacuum so that surface plasmons on either interface will be degenerate. The dotted lines indicate the location of the light line (and the diffracted lines).

The dispersion plot shown in Fig. 14(a) shows that the homogeneous silver layer is not quite optically thick at 64 *nm* as the normal surface plasmon mode has already started to split into the low and high frequency branches. The zeroth order SPP mode does exist, although it is difficult to see as it is very weak and overlaid by the light line. The weakness is a result of the fact that a lamellar grating with very narrow slits is described by a Fourier expansion with very small (in magnitude) lower order Fourier harmonics, therefore, the lower order SPPs are excited only weakly. At $t = 8$ *nm*, as in Fig. 14(b), the modes have split significantly, with the low frequency mode redshifting in frequency while the high frequency mode has blueshifted. There are also higher order $(2k_g, 3k_g \ldots qk_g)$ low frequency modes that have been brought down into view and the high frequency branch appears to have weakenend in strength significantly. By $t = 2$ *nm*, as in Fig. 14(c), the low frequency modes have redshifted further, and the lowest order low frequency mode has weaknened significantly. The high frequency branch does not appear to have moved significantly since $t = 8$ *nm* and has weakened further. When the grating is finally discontinuous ($t = 0$ *nm*), as in Fig. 14(d), many low frequency modes have come down into view. However, note that the high frequency mode appears to have diminished greatly, not by blueshifting as there was no noticeable blueshift below $t = 8$ *nm*, but by weakening until it has very nearly vanished. Also note, from (c) and (d) of Fig. 14, that the lowest order low frequency mode has also weakened and vanished, and that what looks like the lowest order coupled surface plasmon mode is in fact a higher order mode that has been brought down in frequency. Therefore, this structure will support normal coupled surface plasmon modes, however, it only appears to support the low frequency branch of the coupled surface plasmon modes. Furthermore, it does not support the lowest order coupled surface plasmon mode, and that there is a noticeable band gap between modes at $k_x = 0, 1$. This is because the slit, even at only 20 *nm*, is large enough to cause significant perturbation to the normal surface plasmon modes and to prevent the lowest order mode existing.

At first it may be surprising to find that the high frequency coupled SPP mode cannot exist on lamellar gratings, this is because, it must have a shorter wavelength than the low frequency mode, and therefore, it would be expected that each wire would appear more like a planar film to the high frequency mode. However, one has to consider the behaviour of the fields as the grating thickness is reduced. It has been discussed in the Introduction that, the high frequency (short-range) mode is associated with fields that have a larger fraction inside the metal than the

#101954 - $15.00 USD Received 23 Sep 2008; revised 20 Nov 2008; accepted 23 Nov 2008; published 19 Dec 2008

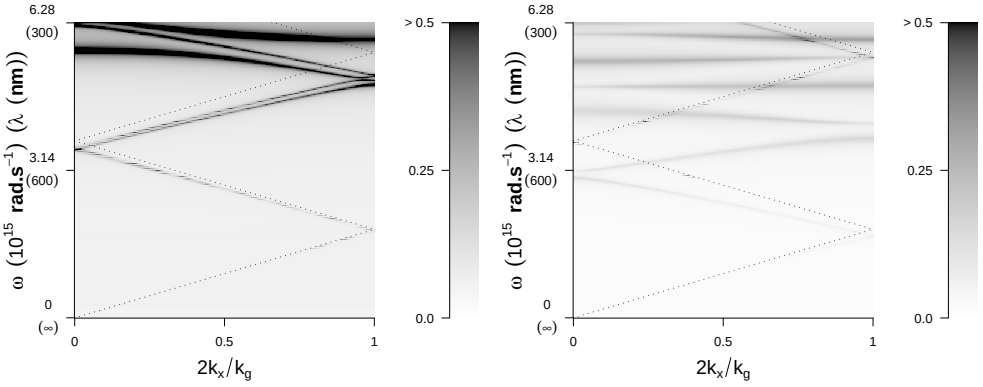

(a) $t = 64\ nm$ (b) $t = 8\ nm$

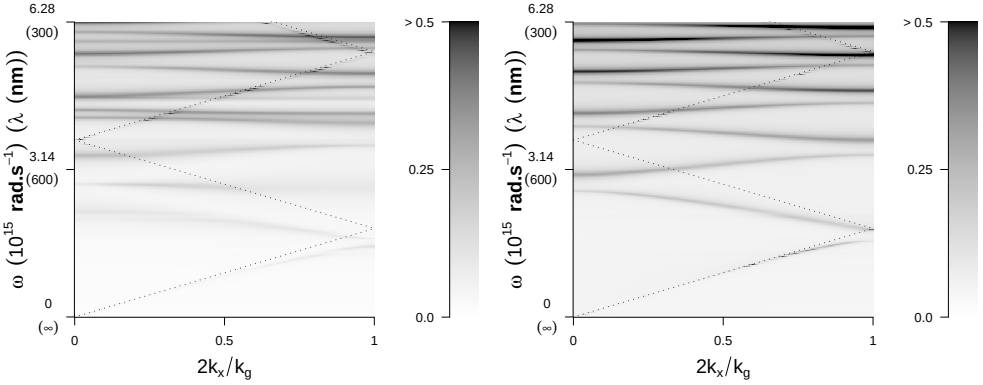

(c) $t = 2\ nm$ (d) $t = 0\ nm$

Fig. 14. Poles of the S matrix of a silver rectangular grating as a function of both the incident frequency and in-plane momentum for decreasing t. The fixed grating parameters are $d = 500\ nm$, $fd = 480\ nm$, $h = 10\ nm$ and the substrate is vacuum. The frequency is in the range $0 < \omega \leq 6.28 \times 10^{15}\ rad.s^{-1}$, giving a wavelength range of $300\ nm \leq \lambda < \infty$, and the in-plane momentum is in the range $0 \leq 2k_x/k_g \leq 1$. The dotted line indicates the light and diffracted lines.

#101954 - $15.00 USD Received 23 Sep 2008; revised 20 Nov 2008; accepted 23 Nov 2008; published 19 Dec 2008

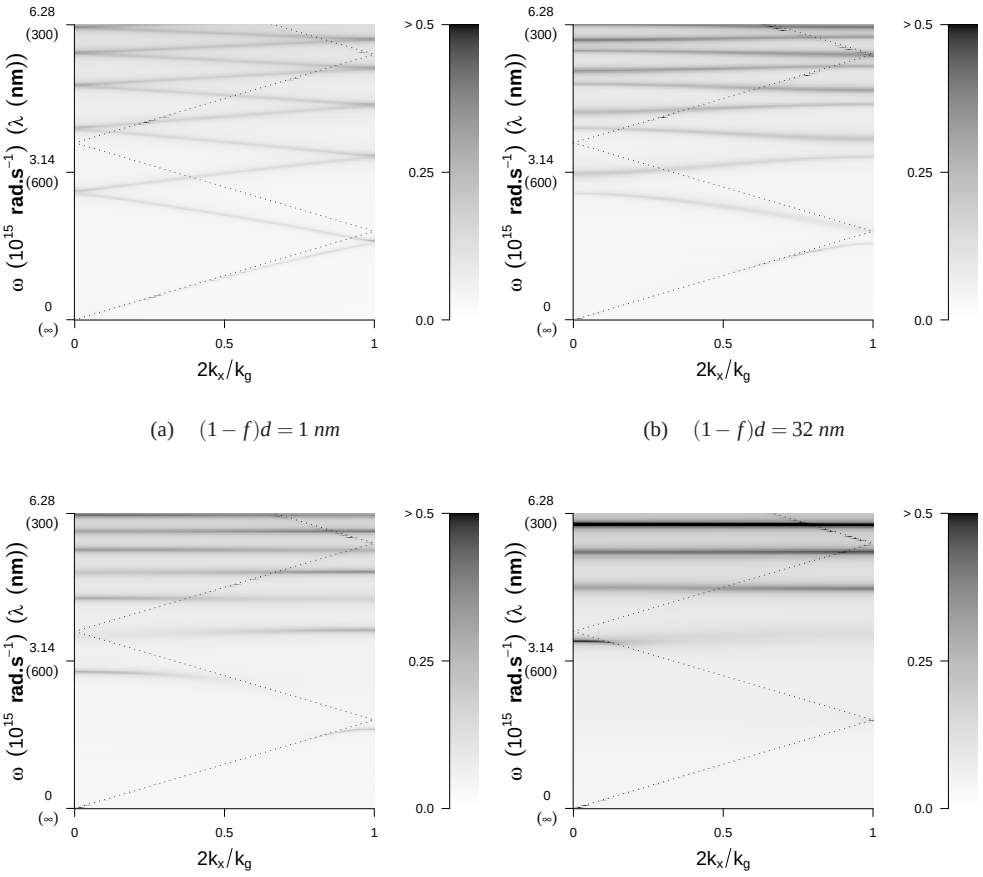

(a) $(1-f)d = 1\ nm$ (b) $(1-f)d = 32\ nm$

(c) $(1-f)d = 128\ nm$ (d) $(1-f)d = 244\ nm$

Fig. 15. Poles of the S matrix of a silver lamellar grating as a function of both the incident frequency and in-plane momentum for increasing slit widths. The fixed grating parameters are $d = 500\ nm$, $h = 10\ nm$ and the substrate is vacuum. The frequency and in-plane momentum ranges are the same as in Fig. 14.

low frequency (long-range) mode, and that, as the film thickness is reduced, this proportion of fields increases. Therefore, the fields associated with the high frequency mode experience the metal to a much greater degree than the low frequency mode, and thus, the mode must be much more significantly perturbed by the presence of the slits than the low frequency mode, or indeed the uncoupled mode. This explains why this mode does not exist on thin lamellar gratings. This can also be considered due to the fact that the high frequency mode occurs at higher frequencies, while the low frequency mode red-shifts. Therefore, the high frequency mode becomes more surface plasma-like, while the low frequency mode becomes more grazing photon-like, which is naturally perturbed much less by the slits.

In order to investigate the perturbation effect on the normal surface plasmon modes that the slits introduce, Fig. 15 shows the dispersion plots for a similar discontinuous grating as in Fig. 14, but the slits of the grating are varied in width.

Figure 15(a) gives the dispersion plot of a similar grating when the slit width is only 1 *nm*.

#101954 - $15.00 USD Received 23 Sep 2008; revised 20 Nov 2008; accepted 23 Nov 2008; published 19 Dec 2008

Although, even at this incredibly small slit width, the mode is still noticeably red-shifted from its normal position (see Fig. 14(a)), its dispersion curve indicates that it has a largely normal character. As for the previous investigation, only the low frequency coupled surface plasmon modes appear to significantly exist on a discontinuous grating, and these have been significantly redshifted from the uncoupled normal surface plasmon frequency due to the low grating height. Therefore, as this is such a small slit width, it appears that only low frequency coupled order modes may exist on a discontinuous grating, regardless of the slit width.

There are also no noticeable bandgaps in the structure, so the very small slits must not be perturbing the surface plasmon propagation along each interface significantly. It should be noted that, unlike in Fig. 14(d), the lowest frequency mode in this dispersion plot is indeed the lowest frequency coupled surface plasmon mode, again, because the very narrow slit causes little perturbation to the coupled surface plasmon mode. As the slits are widened to 32 *nm*, as in Fig. 15(b), the perturbation becomes significant, therefore the surface plasmon modes become significantly perturbed, and band gaps are opened at $k_x = 0, 1$.

Further increases in slit width to 128 *nm* (Fig. 15(c)) results in the family of modes redshifting and flattening more significantly. At the same time the lower order modes also weaken, until finally, at a slit width of 256 *nm* (Fig. 15(d)), they vanish altogether. Then only the very high order modes can exist, because they have an effective wavelength that is short enough such that they are not as strongly perturbed by the slits. From the discussion above, it might be expected that the higher order low frequency (long range) coupled modes do not exist because they occur at similar high frequencies to the lower order high frequency (short range) modes, which have been shown not to exist due to a large fraction of their fields existing within the absorbing metal. However, it is emphasised that these are the higher order *low frequency* coupled modes, therefore, their fields are more excluded from the metal than for the high frequency mode, such that they are less perturbed by the slits, and they can exist even at high frequencies.

It has, therefore, been shown that the normal (lower order) surface plasmon modes cannot exist on discontinuous gratings, with the caveat that the slits in the grating must not be very narrow. The results presented here suggest that, in the optical regime, the slits of the grating must be $\lesssim \lambda/100$ for the surface plasmon polariton to exist, however, even at this narrow slit width, the mode will still be significantly perturbed from its normal location. However, previous work in lower frequency regimes suggest that this constraint does not have to be as severe, for example, in the infra-red regime, unperturbed surface plasmon polaritons have been observed for slits as large as $\sim \lambda/10$. This can be understood by similar dispersion arguments because, the surface plasmon polariton mode, at higher frequencies, has a more surface plasma character, whereas, decreasing the frequency of the surface plasmon polariton causes its character to become more like a grazing photon. Naturally, if the resonance behaves more like a grazing photon then it is going to be less perturbed by the slits. This explains why the slits of a grating can be a larger fraction of the incident wavelength as the frequency of the resonance is decreased.

Figure 16 shows the corresponding reflection efficiency plots for the pole plots of Fig. 15. For the narrowest slit width of 1 *nm* (Fig. 16(a), it can be seen that the normal, although still slightly perturbed, surface plasmon polariton modes may be excited, but as expected, only very weakly. As the slits are broadened, the high reflection horizontal particle plasmon resonance can be seen to appear from very low frequencies, it sharpens and blueshifts in frequency (as expected from Fig. 10), until Fig. 16(c) where the high reflection horizontal particle plasmon mode can clearly be seen. At no point is the resonance affected by the diffraction edge, apart from an expected decrease in reflection efficiency when diffracted orders are present, and so does not appear to be a resonance associated with diffractive coupling. Therefore, Figs. 15 and 16 shows that the horizontal particle plasmon mode appears not to evolve from the normal surface plasmon

#101954 - $15.00 USD Received 23 Sep 2008; revised 20 Nov 2008; accepted 23 Nov 2008; published 19 Dec 2008

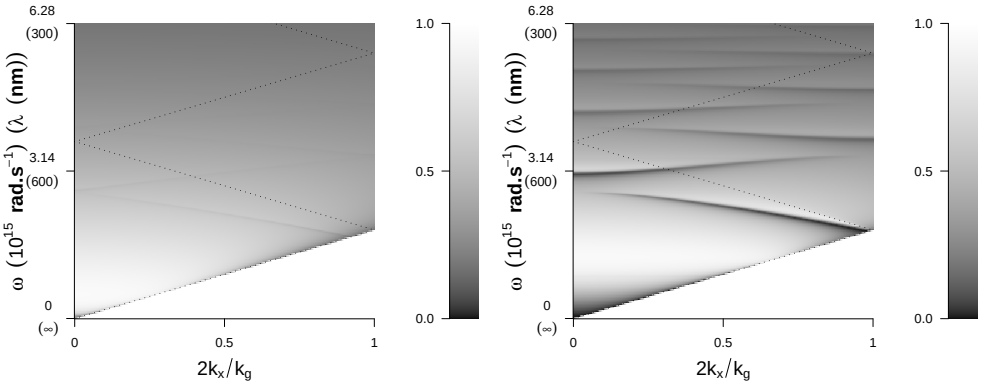

(a) $(1-f)d = 1\ nm$

(b) $(1-f)d = 32\ nm$

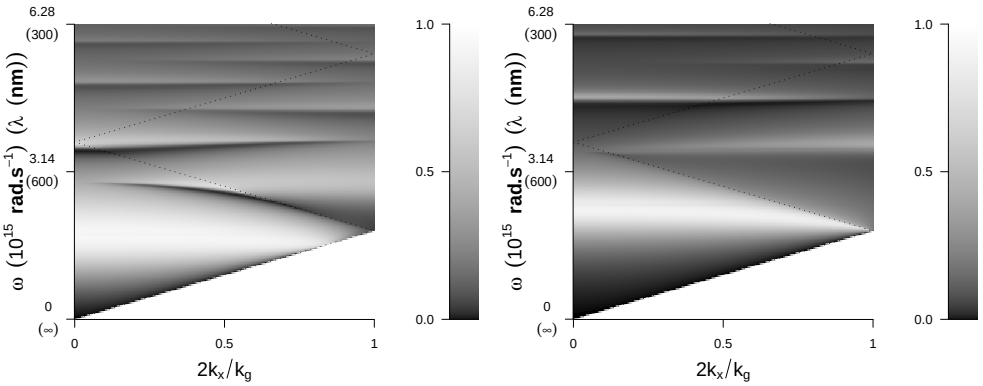

(c) $(1-f)d = 128\ nm$

(d) $(1-f)d = 244\ nm$

Fig. 16. Reflection efficiency response of a silver lamellar grating as a function of both the incident frequency and in-plane momentum for the same increasing slit widths as Fig. 15. The fixed grating parameters are $d = 500\ nm$, $h = 10\ nm$ and the substrate is vacuum. The frequency and in-plane momentum ranges are the same as in Fig. 14.

#101954 - $15.00 USD Received 23 Sep 2008; revised 20 Nov 2008; accepted 23 Nov 2008; published 19 Dec 2008

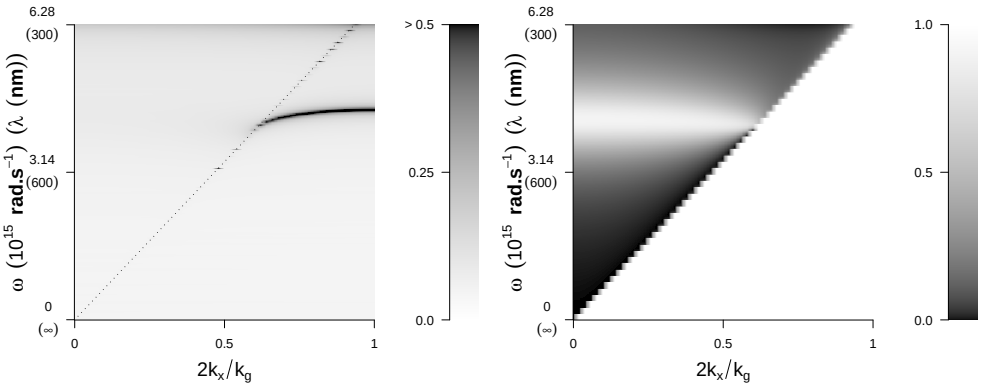

(a) Poles of S matrix (b) Reflection efficiency

Fig. 17. Poles of the S matrix and reflection efficiency response of a silver lamellar grating as a function of both the incident frequency and in-plane momentum. The fixed grating parameters are $d = 140$ *nm*, $f = 0.5$, $h = 10$ *nm* and the substrate is vacuum. The frequency and in-plane momentum ranges are the same as in Fig. 14.

modes, nor does it appear to be related to the periodicity of the structure. However, there also appears to be no pole relating to the horizontal particle plasmon mode.

In order to investigate the evolution of the horizontal particle plasmon mode further, and why there appears to be no associated pole, the investigation of Fig. 14 is repeated for a grating where the resonance is stronger and sharper; this requires a shift back to non-diffractive structures.

First, in Fig. 17 we show the poles of the scattering matrix (a) along with the resulting reflection efficiences (b) for a system where $t = 0$ *nm*, a purely discontinuous structure, with a period 140 *nm*, wire and slit width 70 *nm*, height 10 *nm*, and with a substrate that is vacuum. There is a clear pole beyond the light line that appears to meet the light line at the correct frequency for the reflection peak (the localised coupled horizontal particle plasmon), however, there appears to be no pole in the radiative region.

Figure 18 gives an enlarged line plot of the poles of the scattering matrix when $k_x = 0$ - normal incidence. In fact, as Fig. 18 shows, there is a very weak pole that can be observed at the correct frequency of the resonance. The reason for the weakness of this pole is the spectral broadness of the resonance, this is caused by a high amount of damping that is occuring due to the enhancement and high localisation of the fields around the wires - another similarity with particle plasmons. The pole becomes much sharper to the right of the light line because the radiative damping is removed and hence the resonance and pole become significantly sharper. The localisation of continuous interface surface plasmons decreases in the non-radiative regime because there is an increase of the field penetration into the dielectric. It is expected that a similar reduction in localisation occurs for the resonance presented here and hence there is a dispersion of the mode with k_x beyond the light line.

The switch back to non-diffractive structures allows easier analysis of why there does not appear to be a pole associated with the particle plasmon mode because these yeild simpler dispersion diagrams. Furthermore, when this investigation is carried out for diffractive gratings with narrow slits, such that it would be expected that normal (coupled) surface plasmons and the horizontal particle plasmon may exist on the same structure, the horizontal particle resonance, as shown in Figs. 10, 15(a) and 16(a), would become drastically redshifted away from its normal position. In addition, it would be significantly broadened, and therefore, the associated pole

#101954 - $15.00 USD Received 23 Sep 2008; revised 20 Nov 2008; accepted 23 Nov 2008; published 19 Dec 2008

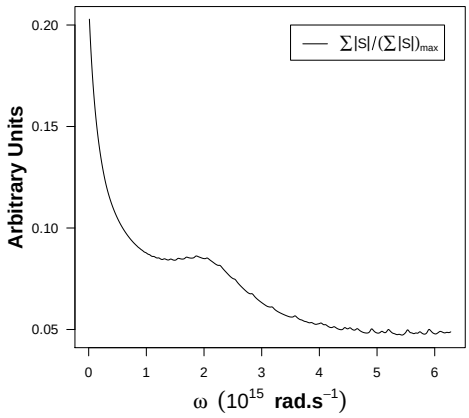

Fig. 18. Poles of the S matrix of a silver lamellar grating as a function of both the incident frequency. The fixed grating parameters are $d = 140$ *nm*, $f = 0.5$, $h = 10$ *nm* and the substrate is vacuum. The frequency range is the same as in Fig. 14 and the in-plane momentum is $k_x = 0$.

would become even less visible. Thus, a similar investigation on diffractive gratings with very narrow slits, where both normal (coupled) surface plasmons and the horizontal particle plasmon modes both exist for $t = 0$ *nm*, is impracticable.

Figure 19 presents the dispersion of the poles for $t = 64, 4, 2, 1$ *nm*. Naturally the plot for $t = 64$ *nm* 19(a) is almost blank before the light line due to the sub-wavelength nature of the structure. At very high frequencies, near the light line, there are some poles that can be seen, this is because, at 64 *nm* the structure is not quite optically thick. Therefore, the evanescent fields of the normal surface plasmon modes, expected at $\lambda = 280$ *nm* for $k_x = k_g/2$, penetrate far enough into the homogeneous region to be able to form coupled surface plasmon modes. Thus, the lower frequency mode of the split k_g-scattered pole has started to come into view. This can also be seen beyond the light line, where the unscattered pole has clearly decreased significantly from its expected location.

The plot for $t = 4$ *nm* (19(b)) shows that this split pole has reduced further in frequency, furthermore, there are clearly the $2k_g, 3k_g \ldots qk_g$ poles that have also split and the low frequency pole has been brought down into view, with the same band flattening as expected from the results above (Fig. 14). The remaining pole plots, $t = 2, 1$ *nm* (19(c) and (d) respectively) show the same behaviour as many more poles come down in frequency as the coupling becomes more extreme. At the same time the poles weaken in strength until for $t = 0$ *nm*, as in Figs. 17 and 15(d), they disappear completely. Here, not even the higher order normal surface plasmon modes may be seen because the wire width is so small that only very high order modes may exist and they are at far too high a frequency to be observed. In fact, they are beyond the frequencies when silver becomes a dielectric and so no normal surface plasmon modes may exist at all in this case.

Beyond the light line there is a pole that, while also reducing in frequency as t is reduced, is reducing much more slowly, and the poles associated with the normal surface plasmon modes pass freely through it without any interaction. Clearly then, the pole does not evolve from normal surface plasmon modes and is in no way related to the normal surface plasmon modes. As discussed previously, this pole is associated with a very weak pole in the radiative zone

#101954 - $15.00 USD Received 23 Sep 2008; revised 20 Nov 2008; accepted 23 Nov 2008; published 19 Dec 2008

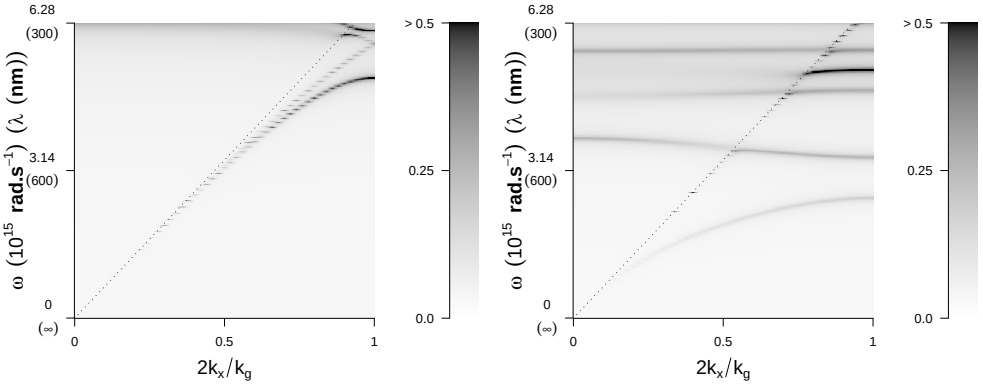

(a) $t = 64\ nm$ (b) $t = 4\ nm$

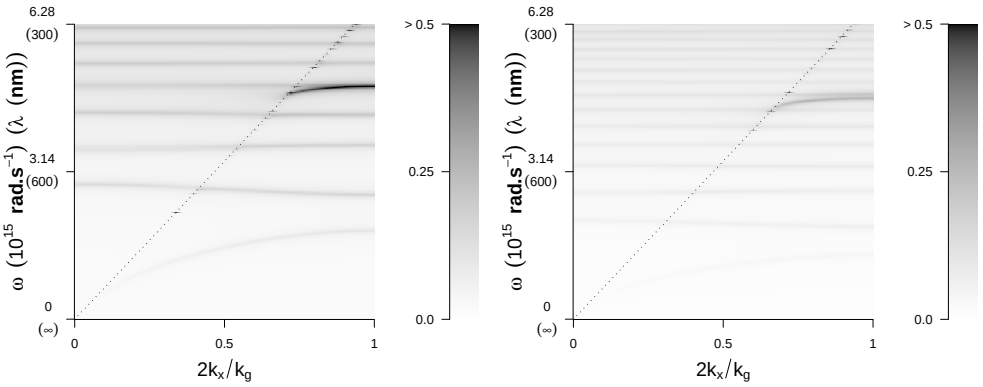

(c) $t = 2\ nm$ (d) $t = 1\ nm$

Fig. 19. Poles of the S matrix of a silver rectangular grating as a function of both the incident frequency and in-plane momentum for decreasing t. The fixed grating parameters are $d = 140\ nm$, $f = 0.5$, $h = 10\ nm$ and the substrate is vacuum. The frequency and in-plane momentum ranges are the same as in Fig. 14.

#101954 - $15.00 USD Received 23 Sep 2008; revised 20 Nov 2008; accepted 23 Nov 2008; published 19 Dec 2008

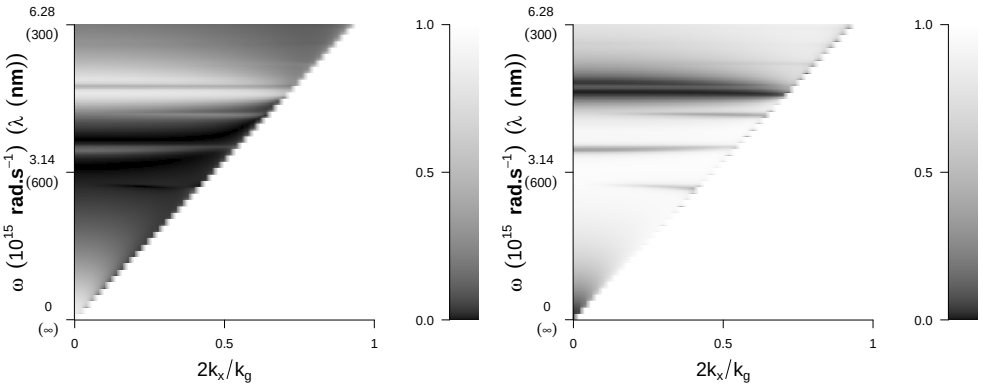

(a) Reflection Efficiency (b) Transmission Efficiency

Fig. 20. Reflection and transmission efficiency responses of a silver rectangular grating as a function of both the incident frequency and in-plane momentum. The fixed grating parameters are $d = 140$ *nm*, $f = 0.5$, $h = 10$ *nm* and the substrate is vacuum. The frequency and in-plane momentum ranges are the same as in Fig. 14, and $t = 2$ *nm*.

that defines the broad high reflection resonance we call a coupled horizontal particle plasmon polariton. A similar investigation can be produced for the uncoupled resonance. Therefore, this result confirms that the horizontal particle plasmon resonance does not evolve from normal surface plasmon modes.

Figure 20 shows the corresponding reflection and transmission efficiencies for the system where $t = 2$ *nm*. The high reflection resonance associated with the coupled horizontal particle plasmon resonance can clearly be seen at a frequency matching the pole beyond the light line, which are both slightly blueshifted by the non-zero t. There is also a series of reflection minima (transmission maxima), one of which coincides with the broad reflection peak, which are associated with the other family of poles. These are the coupled normal surface plasmons and this plot is only shown in order to illustrate that the normal surface plasmon modes are indeed associated with transmission enhancement and, furthermore, when they coincide with the high reflection horizontal particle plasmon resonance, they do not interact in any way and the resultant efficiencies are merely the average of the two resonances - similarly to when the horizontal particle plasmon resonance coincides, but does not interact, with a cavity resonance.

It is now possible to conclusively confirm that the horizontal resonance presented is indeed of a particle plasmon-like nature. Figures 5, 10, 11, 12 and 13 show that the resonance is highly localised to the wires of the grating and independent of the periodicity of the structure, such that the optical response is a superposition of non-interacting wire resonances. This behaviour is analogous to that of an array of independent particle plasmons, and contradictory to the nature of normal diffractively excited surface plasmons. When h is large, the horizontal particle plasmon may only exist on the incidence surface of the wires and the resonance is independent of h because its evanescent decay length is smaller than the height of the grating - the uncoupled (1-dimensional) horizontal particle plasmon polariton. As the grating height is reduced, the evanescent field of the upper horizontal particle plasmon resonance is able to excite a secondary plasmon on the bottom surface of each wire through the metal. As the grating height is reduced further the secondary horizontal particle plasmon is excited more efficiently, and hence the coupling efficiency increases, until eventually, the two resonances become a strongly coupled pair. This results in field enhancement and a redshift of the resonance - the coupled

#101954 - $15.00 USD Received 23 Sep 2008; revised 20 Nov 2008; accepted 23 Nov 2008; published 19 Dec 2008

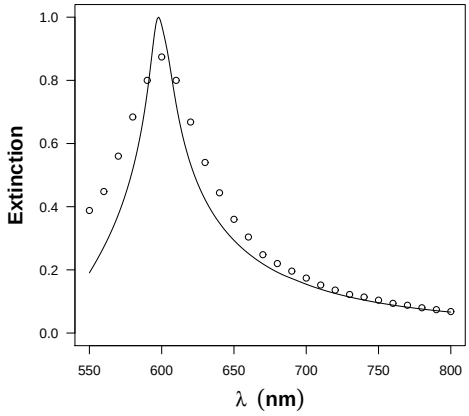

Fig. 21. Experimental data published in Fig. 8(c) of Schider *et. al.* [13] (points), with theoretical calculations using the present model (line). Experimental parameters are given as $d = 350$ *nm*, $h = 25$ *nm*, $f = 0.43$; theoretical parameters are $d = 356$ *nm*, $h = 27$ *nm*, $f = 0.43$.

(2-dimensional) horizontal particle plasmon polariton. At this point the grating is also acting as an inverse polariser as it is reflecting more TM radiation than it transmist, and vice versa for TE radiation.

It is also concluded that the new horizontal particle plasmon modes presented here (coupled and uncoupled) do not evolve from diffractive surface plasmon modes in the same way as localised cavity modes have been shown to. Therefore, they are in no way related to normal surface plasmon modes, in an analogous way to the fact that an array of independent particle plasmons are in no way related to the normal surface plasmon modes that occur on a diffractive array of holes (or other perturbations) in a metal surface. It is a particle-like, resonance that is only ever associated with a significant reflection enhancement. The reflection enhancement also makes this resonance subtly distinct from the particle plasmon resonances previously demonstrated on individual circular (and irregular) cross-section wires.

6. Comparison with experiment

The coupled horizontal particle plasmon resonance has been observed experimentally [13]. This is shown as circles in Fig. 21 (from Fig. 8(c) of [13]), where the $Extinction = log(T_0/T)$ is plotted as a function of incident wavelength, our modelling is the continuous line.

It can clearly be seen that the transmission extinction feature, although broader experimentally, may be modelled. The broadening is expected as a result of the increase of the imaginary part of the permittivity through the 2-dimensional confinement of electrons in the wire, as discussed previously, and also the non-ideal geometry of the wires.

It is instructive to plot the reflection efficiency against grating height for the same parameters as Fig. 21, at a wavelength of 601 *nm*, so that the feature may be presented in a similar manner to Fig. 2; this is done in Fig. 22. The feature is clearly of the same nature as that in Fig. 2, including the higher order peaks at even smaller grating height. Furthermore, the feature is located at the correct grating height for the experimental data. This indicates that the horizontal particle plasmon resonance predicted here, giving high reflection enhancement, is the same resonance that has been observed experimentally by Schider *et. al.* [13]. Field plots for this

#101954 - $15.00 USD Received 23 Sep 2008; revised 20 Nov 2008; accepted 23 Nov 2008; published 19 Dec 2008

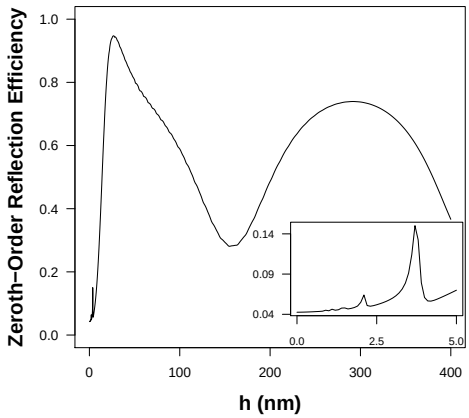

Fig. 22. Reflection efficiency as a function of grating height, for the parameters $d = 356$ *nm*, $f = 0.43$, $\lambda = 601$ *nm*.

response are identical to those in Fig. 5(a) except the maximum field enhancement is slightly smaller.

Note that, although this work has experimentally demonstrated the existence of the particle plasmon-like mode, its nature was not fully explained. Furthermore, although it was hypothesised, but not proved, that this mode may have a dipolar character, it was not realised that the transmission extinction was not a result of scattering, but due to an enhancement in reflection, and therefore, the mode was subtly different to a typical particle plasmon resonance.

7. Conclusions

We have presented models of the response of sub-wavelength lamellar gratings illuminated by radiation whose electric field lies in a plane orthogonal to the grating wires. It has been observed that it is possible to excite two distinct types of resonance. The first resonance is the excitation of a horizontal particle plasmon resonance that is associated with a high reflection efficiency. Beyond approximately $h = 40$ *nm*, this resonance is independent of the grating height. At this point the resonance is essentially a 1-dimensional planar particle plasmon. Below this height, the evanescent field of the resonance is able to penetrate the metal of the grating and couple with a secondary horizontal particle plasmon resonance on the bottom surface of the wires. As the height is reduced further, these resonances become strongly coupled and the response sharpens and redshifts significantly. At this point the resonance is effectively a 2-dimensional particle plasmon. In addition, this resonance still gives a high reflection efficiency below grating heights where a continuous film would start becoming transparent, and indeed does so for radiation with E-field parallel to the wires. Therefore, this resonance allows very thin gratings to respond to different polarisations of incident light in the opposite sense to that which is predicted by the standard wire-grid theory of the restricted motion of electrons. Furthermore, both the coupled and uncoupled modes are highly localised resonances, which may not propagate between wires, and are independent of the grating period (for a constant wire width). The behaviour of normal surface plasmon modes on discontinuous gratings has also been investigated, and how these relate to the normal surface plasmon modes that occur on continuous gratings with a shallow perturbation. It has been shown that the horizontal particle plasmon resonance

#101954 - $15.00 USD Received 23 Sep 2008; revised 20 Nov 2008; accepted 23 Nov 2008; published 19 Dec 2008

presented here does not evolve from normal surface plasmon polaritons and is only particle-like in nature. Furthermore, it is also demonstrated that the resonance is subtly different than the well known particle plasmon mode because the planar structure and periodicity of the resonance causes the re-radiated light to propagate in the same direction as, and is in phase with, the specularly reflected light. This leads to a reflection enhancement not observed before from a particle plasmon resonance. It is also shown that this resonance has been previously observed experimentally by Schider *et. al.* [13].

The second resonance is the excitation of vertical SPPs along the wire surface that bounds each slit. It has been shown that, when the slits are thin enough, these vertical SPPs may couple together significantly across the slit and it is possible to efficiently excite standing waves along the slit - essentially just the classical TEM cavity mode with some subtle differences due to the periodicity of the structure. These standing waves are associated with reflection extinction (transmission enhancement). Similar cavity modes have been modelled previously for both deep continuous surface relief gratings [12] and lamellar gratings in the infra-red [7] and microwave [10] regimes. We show that the cavity modes, excited in the visible spectrum here, behave with changing parameters as is expected from the results of these previous investigations. We also show that, in the extreme case of very narrow slits, the finite conductivity in the optical regime allows incident radiation to be squeezed into slits whose lengths are considerably less ($\lambda/5$) than the wavelength of the radiation in free space.

Finally, in the case of the sub-wavelength discontinuous gratings investigated here, the new horizontal resonance presented, which has been shown to be distinctly different from the normal surface plasmon resonance observed on continuous diffraction gratings as it has a particle-like character, appears to be purely associated with a reduction in transmission, and when the resonance overlaps with a cavity mode (or indeed a normal surface plasmons), there is no transmission enhancement and the resultant transmission efficiency is an average of the two resonances. This implies that when the two resonances coincide there is no interaction between the two, or at least if they do interact, there is a reduction in the transmission efficiency (not an enhancement) compared to that just away from coincidence.

Acknowledgments

The authors would like to acknowledge the Engineering and Physical Sciences Research Council and Sharp Laboratories Europe for their financial support.

#101954 - $15.00 USD Received 23 Sep 2008; revised 20 Nov 2008; accepted 23 Nov 2008; published 19 Dec 2008